β-Cell–Specific IL-2 Therapy Increases Islet Foxp3$^+$Treg and Suppresses Type 1 Diabetes in NOD Mice

Mark C. Johnson,[1] Alaina L. Garland,[1] Sarah C. Nicolson,[2,3] Chengwen Li,[2,3] R. Jude Samulski,[2,3] Bo Wang,[1] and Roland Tisch[1,4]

Interleukin-2 (IL-2) is a critical cytokine for the homeostasis and function of forkhead box p3–expressing regulatory T cells (Foxp3$^+$Tregs). Dysregulation of the IL-2–IL-2 receptor axis is associated with aberrant Foxp3$^+$Tregs and T cell–mediated autoimmune diseases such as type 1 diabetes. Treatment with recombinant IL-2 has been reported to enhance Foxp3$^+$Tregs and suppress different models of autoimmunity. However, efficacy of IL-2 therapy is dependent on achieving sufficient levels of IL-2 to boost tissue-resident Foxp3$^+$Tregs while avoiding the potential toxic effects of systemic IL-2. With this in mind, adeno-associated virus (AAV) vector gene delivery was used to localize IL-2 expression to the islets of NOD mice. Injection of a double-stranded AAV vector encoding IL-2 driven by a mouse insulin promoter (dsAAVmIP-IL2) increased Foxp3$^+$Tregs in the islets but not the draining pancreatic lymph nodes. Islet Foxp3$^+$Tregs in dsAAVmIP-IL2–treated NOD mice exhibited enhanced fitness marked by increased expression of Bcl-2, proliferation, and suppressor function. In contrast, ectopic IL-2 had no significant effect on conventional islet-infiltrating effector T cells. Notably, β-cell–specific IL-2 expression suppressed late preclinical type 1 diabetes in NOD mice. Collectively, these findings demonstrate that β-cell–specific IL-2 expands an islet-resident Foxp3$^+$Tregs pool that effectively suppresses ongoing type 1 diabetes long term.
***Diabetes* 62:3775–3784, 2013**

Type 1 diabetes is a T-cell–mediated autoimmune disease in which the insulin-producing β-cells in the pancreatic islets of Langerhans are destroyed (1–3). Studies in at-risk individuals, type 1 diabetic patients, and NOD mice have shown that the breakdown in β-cell–specific T-cell tolerance is multifactorial, leading to impaired peripheral immunoregulation (1–3). The diabetogenic response is characterized by a progressive but nondestructive infiltration of the islets by CD4$^+$ and CD8$^+$ effector T cells (Teffs), forkhead box p3–expressing Tregs (Foxp3$^+$Tregs), and other immune effectors in NOD mice (4). This innocuous insulitis then progresses to a destructive stage, leading to β-cell depletion and clinical type 1 diabetes. Recently, it has become evident that the transition to destructive insulitis is in part due to impaired islet-resident Foxp3$^+$Tregs in NOD mice (5–8).

Foxp3$^+$Tregs are dependent on interleukin-2 (IL-2) for maintenance of Foxp3 gene expression, survival, proliferation, and suppressor function (9–12). However, unlike conventional T cells, Foxp3$^+$Tregs do not express IL-2 and consequently are dependent on Teffs and dendritic cells as IL-2 sources (12–14). Dysregulation of the IL-2–IL-2 receptor (IL-2R) pathway contributes to the impaired Foxp3$^+$Treg pool in NOD mice and type 1 diabetic patients (15–17). In NOD mice, decreased IL-2 production by Teffs and dendritic cells, a defect mapping to the insulin-dependent diabetes (*Idd3)* locus containing the *Il2* gene, correlates with reduced Foxp3$^+$Treg survival (15–20). Aberrant Foxp3$^+$Treg survival in NOD mice is detected only in the islets and not in the draining pancreatic lymph nodes (PLNs), a site for differentiation of pathogenic Teffs and various Treg subsets (15–17). In contrast, FOXP3$^+$Tregs obtained from peripheral blood of type 1 diabetic patients exhibit deficient IL-2R signaling in vitro, evident by reduced phosphorylation of signal tranducer and activator of transcription 5 (pSTAT5), a transcription factor that regulates Foxp3$^+$Treg-dependent genes (21).

In view of the potent effects of IL-2 on Foxp3$^+$Tregs, recombinant (r)IL-2 therapy has garnered significant interest for the treatment of chronic inflammation, transplantation, and autoimmunity. The pleiotropic and potentially toxic effects resulting from IL-2 stimulation of conventional T cells and other immune effectors has led to systemic administration of low doses of rIL-2. Low-dose rIL-2 therapy exploits the ability of Foxp3$^+$Tregs, which constitutively express CD25 and the corresponding high-affinity IL-2R, to outcompete other immune effectors when IL-2 is limiting (22). Clinical studies have shown that low-dose rIL-2 therapy is protective in graft-versus-host disease and hepatitis C virus–induced vasculitis (23,24). In addition, β-cell autoimmunity is prevented and/or suppressed in NOD mice following treatment with low-dose rIL-2, rIL-2–anti–IL-2 antibody complexes, or a tetracycline-inducible adeno-associated virus (AAV) vector expressing IL-2 systemically by enhancing the Foxp3$^+$Treg pool (16,25–29). A recent phase I/II trial testing rIL-2 and rapamycin in type 1 diabetic patients, however, reported only a transient increase in FOXP3$^+$Tregs (30), possibly reflecting the need for elevated and persistent levels of IL-2. Furthermore, treatment resulted in an increase in activated natural killer (NK) cells and eosinophils and an accelerated loss of insulin C-peptide levels, suggesting exacerbated β-cell autoimmunity. These clinical findings highlight the potential therapeutic benefit as well as the difficulty in achieving a balance between efficacy and the unwanted pleiotropic and systemic activity of IL-2.

From the [1]Department of Microbiology and Immunology, University of North Carolina at Chapel Hill, Chapel Hill, North Carolina; the [2]Gene Therapy Center, University of North Carolina at Chapel Hill, Chapel Hill, North Carolina; the [3]Department of Pharmacology, University of North Carolina at Chapel Hill, Chapel Hill, North Carolina; and the [4]UNC Lineberger Comprehensive Cancer Center, University of North Carolina at Chapel Hill, Chapel Hill, North Carolina.
Corresponding author: Roland Tisch, rmtisch@med.unc.edu.
Received 25 April 2013 and accepted 16 July 2013.
DOI: 10.2337/db13-0669
This article contains Supplementary Data online at http://diabetes.diabetesjournals.org/lookup/suppl/doi:10.2337/db13-0669/-/DC1.

Accordingly, we have assessed the use of AAV vectors to increase local IL-2 levels in the islets and enhance the resident Foxp3$^+$Treg pool in vivo. AAV vectors are nonreplicating, noncytopathic, nonintegrating, and arguably the most effective and safe strategy to deliver genes in vivo (31). Indeed, AAV vectors have been successfully applied in the clinic to complement various genetic disorders (32–34). AAV vectors transduce both dividing and nondividing cells, and the availability of several serotypes and newly engineered vectors permit targeting of a broad range of cell types and tissues in vivo. Furthermore, selective transgene expression can be achieved with cell-specific promoters (35,36). Coupled with the development of self-complementary or double stranded (ds)AAV vectors (37,38), as well as the recent advances in manufacturing and purification, AAV vectors provide an approach to sustain long-term transgene expression in vivo. In the current study, we demonstrate that dsAAV vector–mediated IL-2 expression by β-cells selectively increases the frequency and function of islet Foxp3$^+$Tregs to effectively suppress type 1 diabetes long-term.

RESEARCH DESIGN AND METHODS

Mice. NOD/LtJ, NOD.CB17-Prkdcscid/J (NOD.*scid*), NOD.Cα$^{-/-}$, NOD.BDC (39), NOD.BDC.Foxp3^{GFP} (40), and NOD.8.3 (41) mice were bred and maintained under specific pathogen-free conditions in an American Association for Laboratory Accreditation–accredited animal facility. NOD mice were diagnosed as diabetic after three consecutive blood glucose readings >250 mg/dL. All procedures were approved by the University of North Carolina Animal Use and Care Committee.

dsAAV vector engineering, packaging, and vaccination. Full-length cDNA encoding murine *Il2* (of the NOD genotype) and *EGFP* were subcloned into a dsAAV plasmid (37) containing the murine preproinsulin II promoter (mIP). dsAAV vector packaging was carried out as previously described (42). Briefly, HEK 293T cells were cotransfected via polyethyleneimine with adeno helper plasmid (pXX6–80), AAV8 capsid plasmid, and dsAAVmIP-IL2/enhanced green fluorescent protein (EGFP) plasmid. Nuclear fractions were harvested 72 h posttransfection and packaged vector purified with a Cesium Chloride (RPI Corp.) gradient. Vector containing fractions and titers were determined by Southern dot blot. NOD mice were vaccinated intraperitoneally with dsAAV8mIP-IL2 or dsAAV8mIP-EGFP.

ELISA. The anti–IL-2 antibody set (JES6-1 and JES6-5; eBioscience) was used at a concentration of 2 μg/mL on a high binding ELISA plate (Costar) to measure IL-2 levels in serum and islet cultures. Interferon-γ (IFN-γ) was measured with the mouse IFN-γ ELISA set (BD optEIA; BD Biosciences) as per the manufacturer's recommendations.

Islet isolation and streptozotocin treatment. Pancreases were perfused with 2 mg/mL collagenase P (Roche) and digested for 30 min at 37°C. Islets were purified via Ficoll gradient, handpicked, and counted. For flow cytometry analysis, lymphocytes were collected from freshly isolated islets after culturing in RMPI complete medium for a minimum of 4 h at 37°C and filtered through a 70-micron nylon mesh.

NOD mice were treated intraperitoneally with 200 mg/kg of streptozotocin (STZ; Sigma-Aldrich), resuspended in fresh sodium citrate buffer (pH 4.0), and 72 h later vaccinated intraperitoneally with AAV8mIP-IL2 or left untreated. Blood glucose levels and serum IL-2 were assessed over 10 days post–rAAV vector vaccination.

Flow cytometry. Cells from various tissues were stained with previously titrated fluorochrome-conjugated monoclonal antibodies specific for: CD3 (145-2C11), CD4 (GK1.5), CD8 (Ly-2), CD25 (PC61.5), CD62L (MEL-14), glucocorticoid-induced tumor necrosis factor receptor–related protein (GITR, DTA-1), inducible costimulator (ICOS, 7E.17G9), cytotoxic T lymphocyte–associated antigen-4 (CTLA-4, UC10-4F10-11), and Foxp3 (FJK-16s). Fc receptors were blocked with rat anti-mouse CD16/32 (2.4G2; BD Biosciences) prior to staining. Intracellular KI67 (B56; BD Biosciences) and Bcl-2 (3F11; BD Biosciences) staining was done using the Fix/Perm and Perm/Wash reagents (eBioscience) according to the manufacturer's recommendations.

Intracellular cytokine staining was performed on single-cell suspensions as previously described (43). Briefly, lymphocytes were stimulated with 500 ng/mL phorbol myristic acid (Sigma-Aldrich) and 1,000 ng/mL ionomycin (Sigma-Aldrich) in complete RPMI medium for 5 h at 37°C and then treated with 10 μg/mL brefeldin A (Sigma-Aldrich) for 4 h. Cells were stained for surface molecules, fixed, and permeabilized with Cytofix/Cytoperm (BD Biosciences) and stained for intracellular IFN-γ (XMG1.2) or IL-10 (JES5-16E3). For pSTAT5 staining, tissues were immediately processed in PBS containing 2% paraformaldehyde. Single-cell suspensions were incubated on ice for 20 min, centrifuged, and resuspended in ice-cold methanol for 30 min. Cells were then counted, washed twice in 1% BSA in PBS, and stained with anti-pSTAT5 antibody (47/Stat5 [pY694]; BD Biosciences) for 1 h on ice. Data were acquired on a Cyan flow cytometer (DakoCytomation) and analyzed using Summit software (DakoCytomation).

In vitro suppressor assay. Islets were pooled from NOD.BDC.Foxp3^{GFP} mice vaccinated with 2.5×10^{10} vector particles (VPs) of AAV8mIP-IL2 or AAV8-mIP-EGFP, and single-cell suspensions stained with CD4- and CD3-specific antibodies in PBS supplemented with 2.5% BSA and 2 mmol/L EDTA. CD4$^+$CD3$^+$GFP$^+$ Tregs were sorted on a MoFlo sorter (DakoCytomation). For T cell responders, naive CD4$^+$CD62L$^+$ splenocytes were isolated from NOD.BDC mice using the CD4$^+$CD62L$^+$ T cell isolation kit II (Miltenyi Biotec) and labeled with Cell Trace Violet (Invitrogen) as per the manufacturer's recommendations. Cell purity in naive populations was >95% by flow cytometry. Splenocytes from NOD.Cα$^{-/-}$ mice pulsed with 1 μg/mL sBDC mimetic peptide were used as antigen-presenting cells (APCs). Naive BDC CD4$^+$ T cells (2.5×10^4), APCs (2.5×10^4), and varying ratios of Foxp3$^+$Tregs were cocultured in complete RPMI medium for 72 h and proliferation of BDC CD4$^+$ T cells assessed by dilution of Cell Trace Violet via flow cytometry.

RESULTS

β-Cell–expressed IL-2 increases islet Foxp3$^+$Tregs. To target transgene expression to β-cells, dsAAV8mIP-IL2 encoding IL-2 driven by mIP was engineered. The serotype capsid 8 protein used to package the AAV vector has β-cell–specific tropism (35,36). IL-2 was detected in cultures of islets prepared from NOD.*scid* mice injected intraperitoneally with dsAAV8mIP-IL2, confirming ectopic IL-2 expression by β-cells in vivo (Fig. 1*A*). No IL-2 was observed in supernatants from single-cell suspensions of liver or heart (data not shown), which are major tissues transduced in vivo by AAV8 vectors (44). Persistent low levels of IL-2 were detected in the serum of 10–12-week-old NOD female mice treated with dsAAV8mIP-IL2 (Fig. 1*B*). Reduction of β-cell mass by STZ injection prior to dsAAV8-mIP-IL2 vaccination significantly decreased serum IL-2 levels (Fig. 1*C*), further indicating ectopic IL-2 expression by β-cells in vivo. No difference in the frequency of conventional CD4$^+$ and CD8$^+$ T cells, B cells (CD19$^+$B220$^+$), and NK cells (DX5$^+$) was detected in the blood of dsAAV8mIP-IL2–vaccinated animals compared with control groups (Fig. 1*D*).

The effect of increased local IL-2 on islet and PLN Foxp3$^+$Tregs was examined in 12-week-old NOD female mice 4 weeks after dsAAV8mIP-IL2 treatment. The frequency and number of islet Foxp3$^+$Tregs were increased up to two-fold in NOD mice treated with dsAAV8mIP-IL2 compared with animals injected with dsAAV8mIP-EGFP or left untreated (Fig. 2*A* and *B*). Notably, no significant effect on PLN Foxp3$^+$Tregs was detected after treatment (Fig. 2*A* and *B*), suggesting that dsAAV8mIP-IL2 administration preferentially affected islet Foxp3$^+$Tregs.

Phenotypic analyses demonstrated that the frequency of islet CD62L^{HI}Foxp3$^+$Tregs was significantly increased in dsAAV8mIP-IL2–treated versus control animals (Fig. 2*C*). In addition, the level of CD25 expression by islet Foxp3$^+$Tregs, based on mean fluorescence intensity, was elevated in a dsAAV8mIP-IL2 dose-dependent manner (Fig. 2*A* and *D*). In contrast, the frequency of islet Foxp3$^+$Treg-expressing CTLA-4, GITR, and ICOS and the levels of expression of the respective molecules were similar between the dsAAV8mIP-IL2 and control groups (Supplementary Fig. 1). Unlike the islets, the phenotype

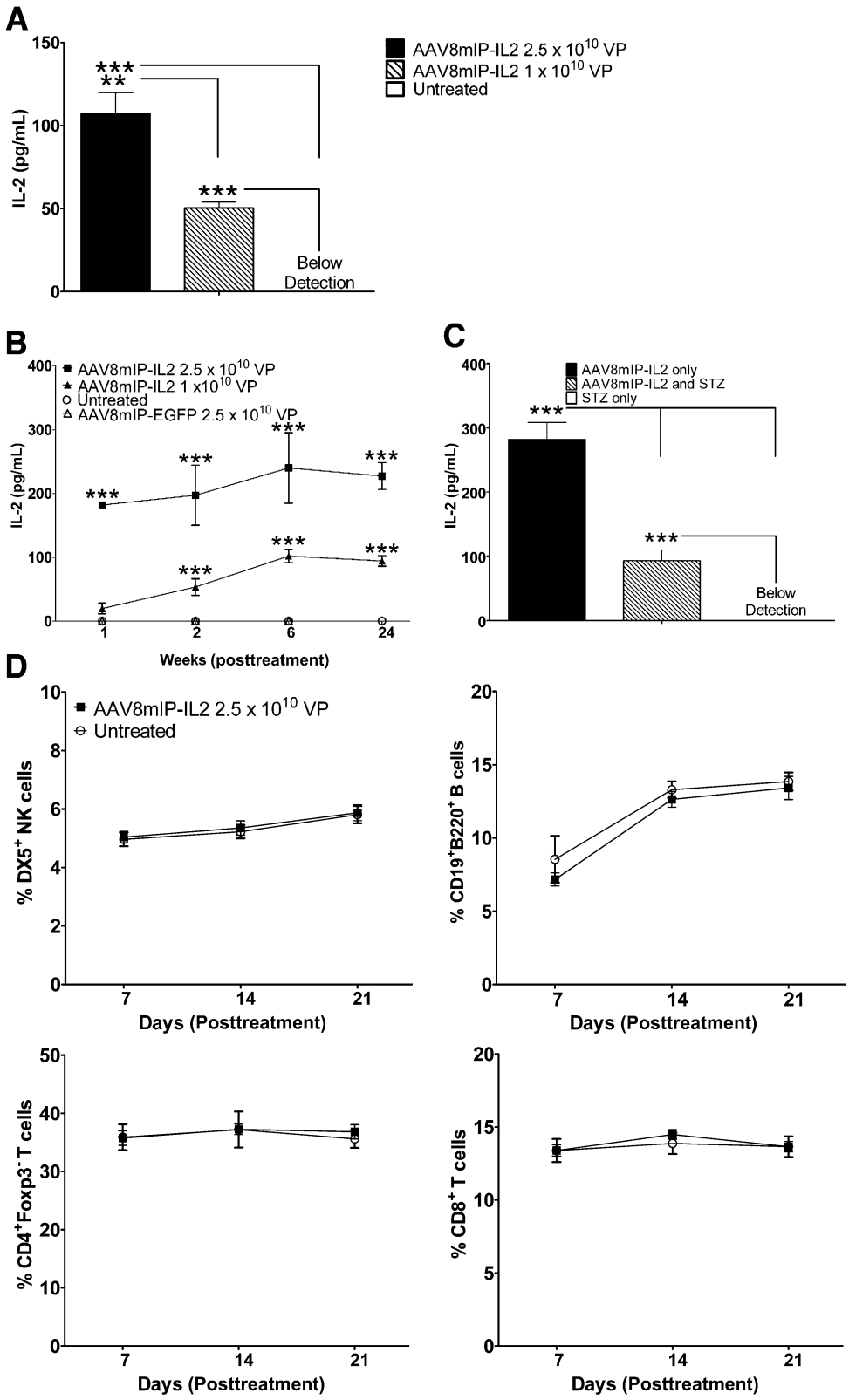

FIG. 1. In vivo β-cell expression of IL-2 after dsAAV8mIP-IL2 injection. *A*: IL-2 levels in supernatants from islets isolated from NOD.*scid* mice treated with dsAAV8mIP-IL2 or left untreated. **$P < 0.01$, ***$P < 0.001$, one-way ANOVA ± SEM. *B*: Temporal measurement of serum IL-2 from 10–12-week-old NOD female mice ($n = 5$) treated with dsAAV8mIP-IL2, dsAAV8mIP-EGFP, or left untreated. ***$P < 0.001$, two-way ANOVA ± SEM. *C*: Serum IL-2 levels in NOD mice ($n = 5$) treated with STZ alone, STZ plus AAV8mIP-IL2 (2.5×10^{10} VPs) 72 h later, or AAV8mIP-IL2 (2.5×10^{10} VPs) alone at day 10 post–STZ injection. ***$P < 0.001$, two-way ANOVA ± SEM. *D*: Frequency of immune effector cells in peripheral blood of NOD mice left untreated or treated with dsAAV8mIP-IL2 7, 14, and 21 days later. STZ, streptozotocin.

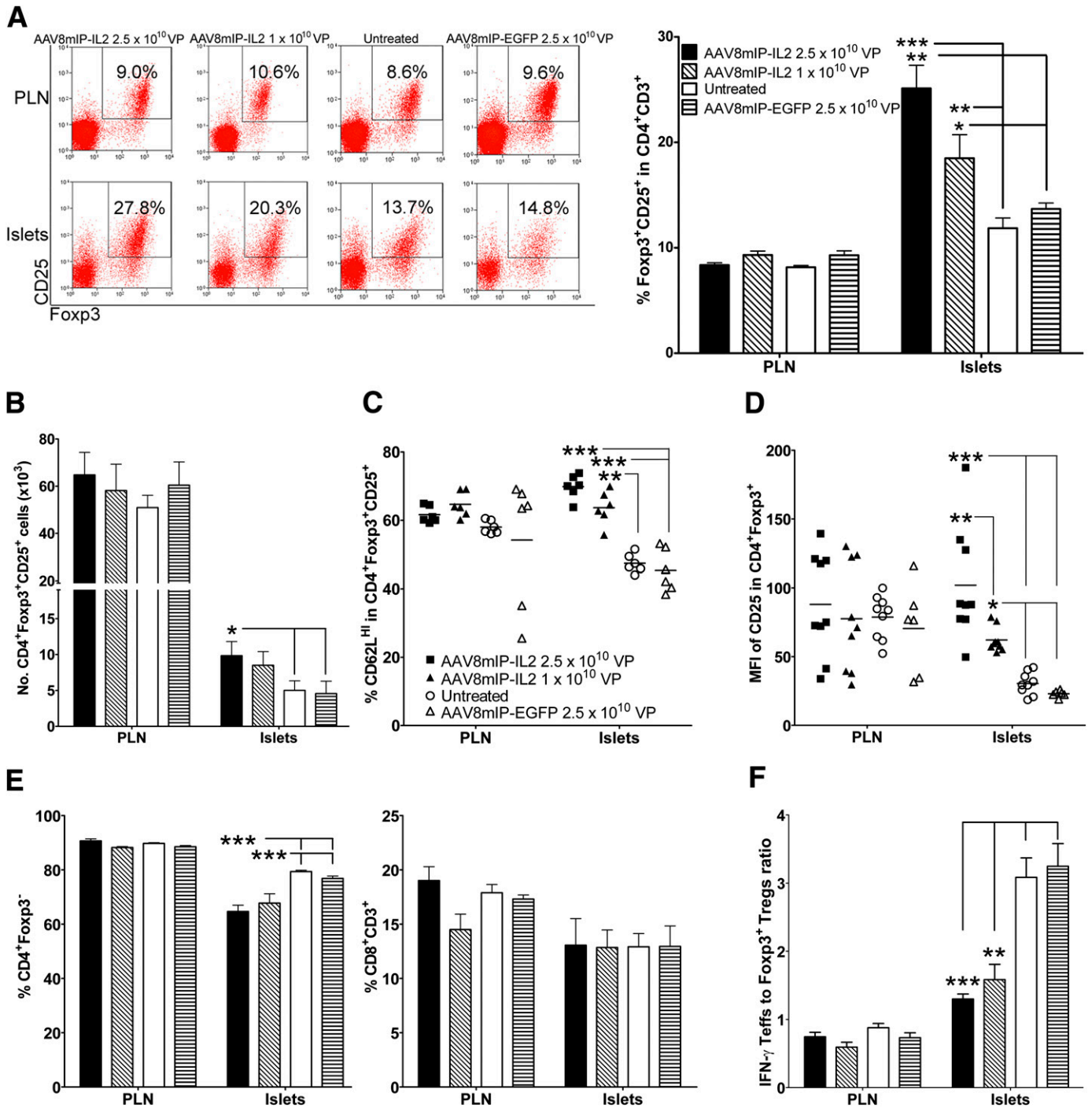

FIG. 2. The frequency and number of islet Foxp3$^+$Tregs are increased after short-term dsAAV8mIP-IL2 treatment. *A*: CD3$^+$CD4$^+$ T cells were gated on and the frequency of Foxp3$^+$CD25$^+$CD4$^+$ T cells in the PLNs and islets of groups of 6–10 NOD female mice 4 weeks posttreatment with dsAAV8mIP-IL2, dsAAV8mIP-EGFP, or left untreated. *$P < 0.05$, **$P < 10^{-2}$, ***$P < 10^{-3}$, two-way ANOVA ± SEM. *B*: Number of islet Foxp3$^+$CD25$^+$CD4$^+$ T cells recovered from 70–100 islets/mouse. *$P < 0.05$, two-way ANOVA ± SEM. Frequency of CD62L^{HI} (*C*) and CD25 mean fluorescence intensity (MFI) (*D*) of Foxp3$^+$Tregs in NOD mice from *A*. *$P < 0.05$, **$P < 10^{-2}$, ***$P < 10^{-3}$, two-way ANOVA ± SEM. Frequency of Foxp3$^-$CD4$^+$ and CD8$^+$ T cells (*E*) and the ratio of IFN-γ$^+$ Teffs to Foxp3$^+$Tregs in the PLN and islets (*F*) of the respective treatment groups. **$P < 10^{-2}$, ***$P < 10^{-3}$, two-way ANOVA ± SEM.

of PLN Foxp3$^+$Tregs was unaffected by dsAAV8mIP-IL2 vaccination (Fig. 2).

In contrast to islet Foxp3$^+$Tregs, no change in the number of conventional IFN-γ$^+$CD4$^+$ and CD8$^+$ Teffs was detected in the islets of dsAAV8mIP-IL2–treated NOD mice (Fig. 2*E*). However, the ratio between the pool of IFN-γ$^+$ Teffs and Foxp3$^+$Tregs in the islets but not PLNs was decreased in dsAAV8mIP-IL2 versus untreated and dsAAV8mIP-EGFP cohorts (Fig. 2*F*).

To determine if the increased islet Foxp3$^+$Treg pool correlated with elevated IL-2R signaling, levels of pSTAT5 were measured. Up to 50% of islet Foxp3$^+$Tregs were pSTAT5$^+$, reflecting an ~10-fold increase in dsAAV8mIP-IL2 versus control groups (Fig. 3*A*). Only a modest two-fold

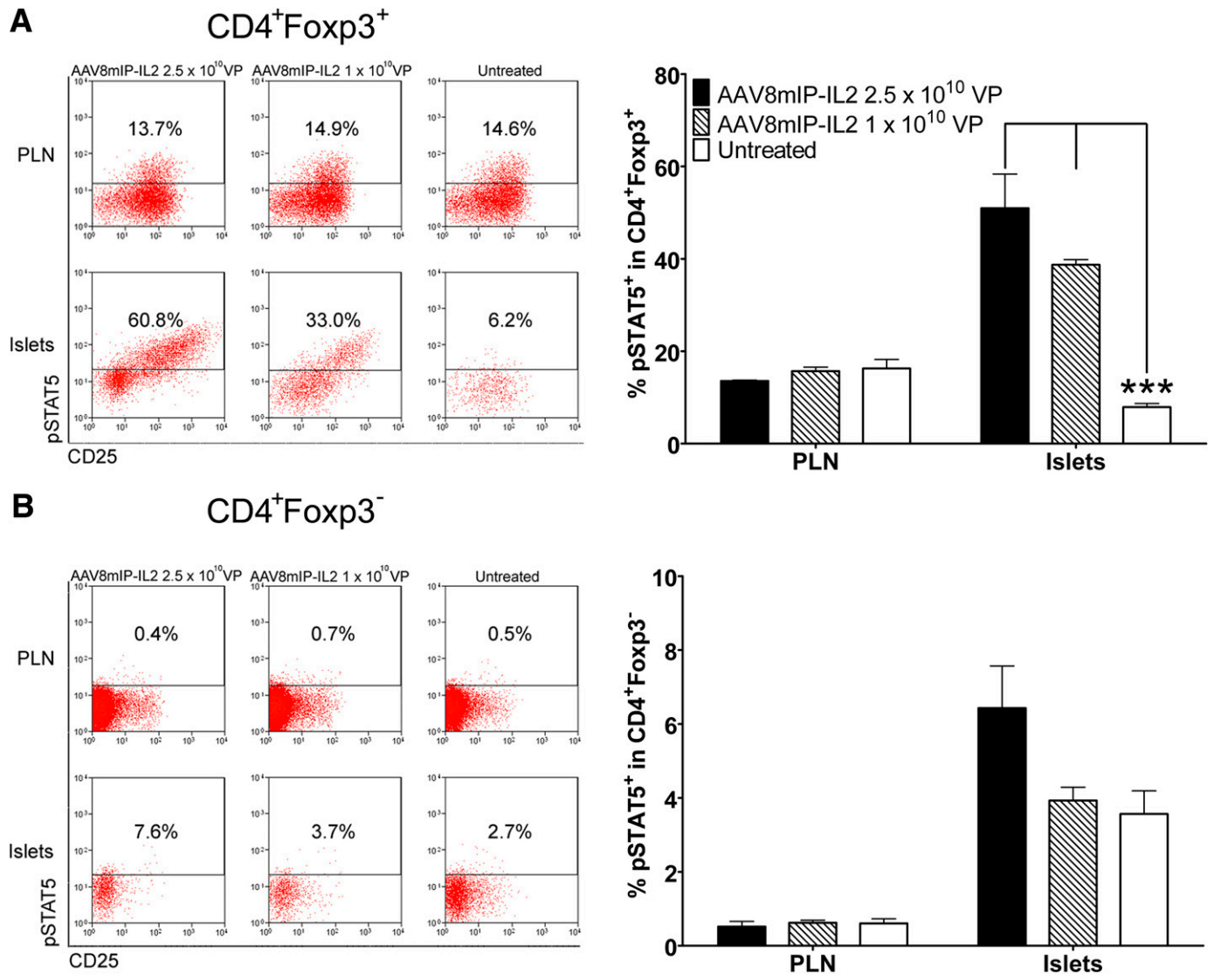

FIG. 3. dsAAV8mIP-IL2 increases the frequency of pSTAT5-expressing islet Foxp3$^+$Tregs. CD3$^+$CD4$^+$ T cells were gated on and the frequency of pSTAT5$^+$ islet and PLN Foxp3$^+$CD4$^+$ (*A*) and Foxp3$^-$CD4$^+$ (*B*) T cells in 10–12-week-old NOD female mice (n = 5) 4 weeks posttreatment with AAV8mIP-IL2 or left untreated determined. ***$P < 10^{-3}$, two-way ANOVA ± SEM.

increase in the frequency of pSTAT5$^+$ cells was detected in conventional Foxp3$^-$CD4$^+$ T cells in the islets of NOD mice vaccinated with 2.5×10^{10} VPs dsAAV8mIP-IL2 (6.4 ± 1.1%) relative to control animals (3.6 ± 0.6%) (Fig. 3*B*). In contrast, levels of pSTAT5 detected in Foxp3$^+$Tregs or Foxp3$^-$CD4$^+$ T cells in the PLNs were unaffected by β-cell–specific IL-2 (Fig. 3). Together, these findings demonstrate that β-cell–specific IL-2 expression results in an increased pool of phenotypically distinct islet but not PLN Foxp3$^+$Tregs marked by elevated IL-2R signaling.

β-Cell–expressed IL-2 enhances the fitness of islet Foxp3$^+$Tregs. Enhanced survival and/or expansion of Foxp3$^+$Tregs may explain the increased islet Foxp3$^+$Treg pool in dsAAV8mIP-IL2–treated animals. To determine if AAV8mIP-IL2 vaccination increased islet Foxp3$^+$Treg survival, expression of the antiapoptotic protein Bcl-2 was measured. The level of Bcl-2-expression following dsAAV8mIP-IL2 treatment was increased in islet Foxp3$^+$Tregs (Fig. 4*A*) and a trend toward an elevated frequency of Bcl-2$^+$ Foxp3$^+$Tregs observed (Fig. 4*B*). In contrast, Bcl-2 expression was unaffected in PLN Foxp3$^+$Tregs (Fig. 4*A* and *B*) or in islet IFN-γ$^+$CD4$^+$ and CD8$^+$ Teffs (Fig. 4*C*).

Proliferation of islet and PLN Foxp3$^+$Tregs after dsAAV8mIP-IL2 administration was analyzed by KI67 staining. The frequency of KI67$^+$Foxp3$^+$CD25$^+$ T cells was significantly increased in the islets by 8 days post–dsAAV8mIP-IL2 treatment (Fig. 4*D*). In contrast, the frequency of KI67$^+$Foxp3$^+$CD25$^+$ T cells in the PLNs remained unchanged over time (Fig. 4*D*), as was the frequency of KI67-staining islet IFN-γ$^+$CD4$^+$ and CD8$^+$ Teffs (Fig. 4*E*).

Next, the influence of β-cell–specific IL-2 on islet Foxp3$^+$Treg suppressor activity was assessed. NOD.BDC mice transgenic for a Foxp3–internal ribosome entry site–GFP reporter cassette (NOD.BDC.Foxp3^{GFP}) were vaccinated with dsAAV8mIP-IL2 or dsAAV8mIP-EGFP and GFP$^+$Foxp3$^+$Tregs sorted from the islets 4 weeks later. The capacity of the respective Foxp3$^+$Tregs to suppress Cell Trace Violet–labeled naive BDC CD4$^+$ T cells following stimulation by peptide-pulsed APC was then measured. Islet Foxp3$^+$Tregs from dsAAV8mIP-IL2–treated NOD.BDC.Foxp3^{GFP} mice

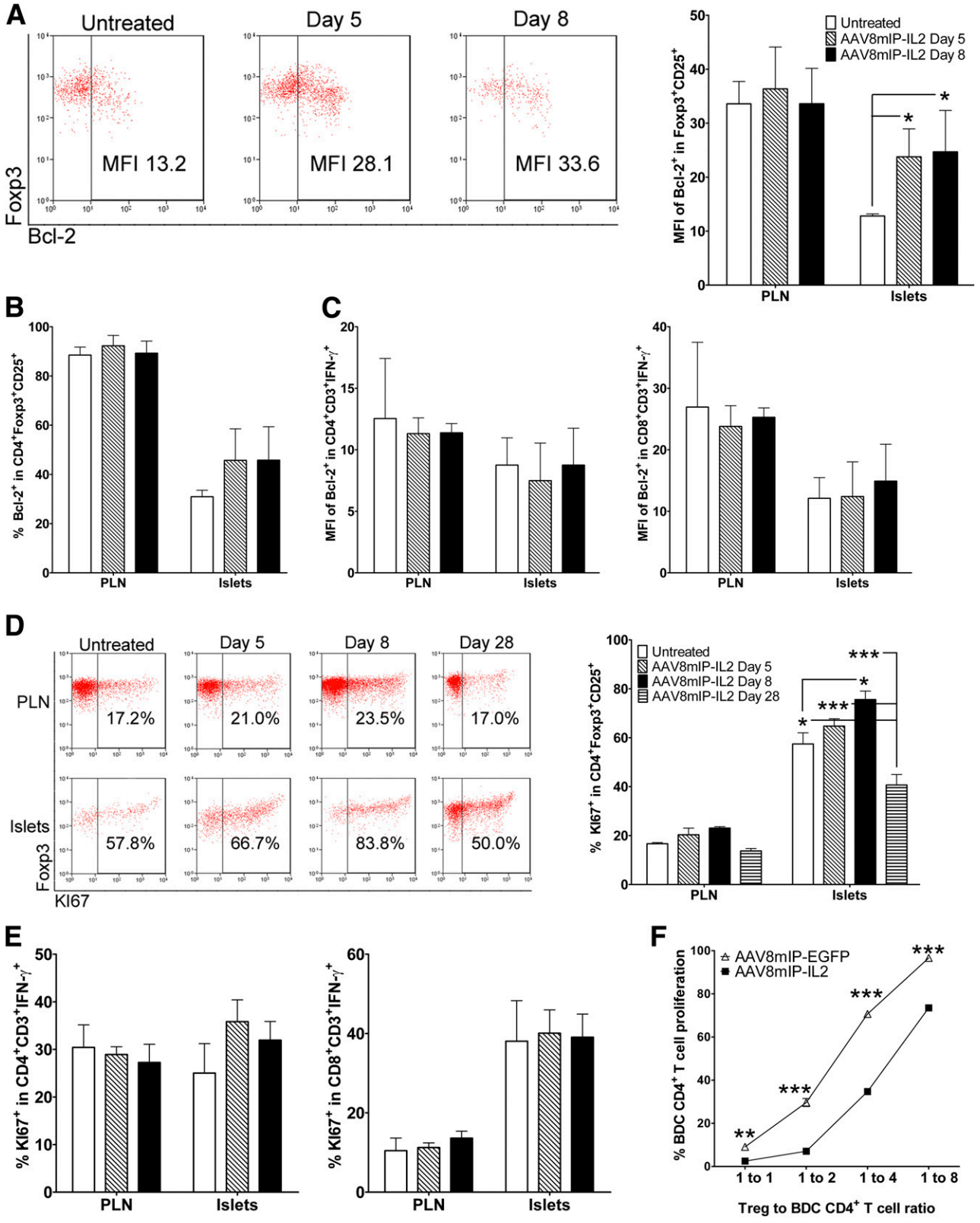

FIG. 4. dsAAV8mIP-IL2 increases expansion and survival of islet Foxp3$^+$Tregs. Foxp3$^+$CD25$^+$CD4$^+$ T cells in the PLNs and islets of NOD female mice (n = 5) treated with AAV8mIP-IL2 (2.5×10^{10} VPs) or left untreated were assessed for the level (*A*) and frequency (*B*) of Bcl-2 expression. *$P < 0.05$, two-way ANOVA ± SEM. *C*: Bcl-2 expression for IFN-γ$^+$CD3$^+$CD4$^+$ and IFN-γ$^+$CD3$^+$CD8$^+$ Teffs in the PLNs and islets at days 5 and 8 posttreatment with AAV8mIP-IL2 or in untreated NOD mice (n = 5). The frequency of KI67$^+$Foxp3$^+$CD25$^+$CD4$^+$ T cells (*D*) and KI67$^+$ IFN-γ$^+$Teffs in the PLN and islets (*E*). *$P < 0.05$, ***$P < 10^{-3}$, two-way ANOVA ± SEM. *F*: In vitro proliferation of Cell Trace–labeled BDC CD62L$^+$CD4$^+$ T cells cocultured with peptide-pulsed APCs and various ratios of GFP$^+$CD3$^+$CD4$^+$ T cells isolated from pooled islets of AAV8mIP-IL2 (2.5×10^{10} VPs) or AAV8mIP-EGFP–treated (2.5×10^{10} VPs) NOD.BDC.Foxp3^{GFP} mice. **$P < 10^{-2}$, ***$P < 10^{-3}$, two-way ANOVA ± SEM. MFI, mean fluorescence intensity.

exhibited significantly increased suppressor activity compared with islet Foxp3$^+$Tregs isolated from dsAAV8mIP-EGFP donors at all ratios tested (Fig. 4*F*). Together, these results demonstrate that β-cell–specific IL-2 enhances the fitness of islet Foxp3$^+$Tregs characterized by increased Bcl-2 expression, proliferation, and suppressor function.

Type 1 diabetes is prevented at a late preclinical stage in NOD mice by β-cell–expressed IL-2. Since β-cell–specific IL-2 expression increased islet Foxp3$^+$Tregs, the efficacy of AAV8mIP-IL2 to suppress ongoing β-cell autoimmunity and prevent overt diabetes was examined. NOD female mice 12 or 16 weeks of age, representing late preclinical stages of type 1 diabetes, received a single intraperitoneal injection of dsAAV8mIP-IL2, dsAAV8mIP-EGFP, or were left untreated, and diabetes was monitored. All NOD female mice treated with 2.5×10^{10} VPs of dsAAV8mIP-IL2 at either 12 or 16 weeks of age remained diabetes-free (Fig. 5*A* and *B*). Similarly, the frequency of diabetes was significantly reduced in NOD female mice treated at 12 weeks of age with 1×10^{10} VPs of dsAAV8mIP-IL2 (2 of 8) relative to animals left untreated (18 of 22) or receiving 2.5×10^{10} VPs dsAAV8mIP-EGFP (10 of 10) (Fig. 5*A*). The latter indicated that diabetes protection was not attributed to a nonspecific effect of dsAAV vector transduction of β-cells.

Diabetes-free NOD mice at 35 weeks of age exhibited a higher frequency of islet Foxp3$^+$Tregs in dsAAV8mIP-IL2 versus control groups, while no marked difference in the PLNs was observed (Fig. 5*C*). Furthermore, islet Foxp3$^+$Tregs of dsAAV8mIP-IL2–treated NOD mice were characterized by an increased frequency of CD62L^{HI} Foxp3$^+$Tregs (Fig. 5*D*). Additionally, the ratio of IFN-γ$^+$ Teffs to Foxp3$^+$Tregs was decreased in the islets of dsAAV8mIP-IL2–treated NOD mice compared with normoglycemic untreated controls (Fig. 5*E*). No difference, however, was detected in the IFN-γ$^+$ Teffs to Foxp3$^+$Tregs ratio for PLN of dsAAV8mIP-IL2–vaccinated animals (Fig. 5*E*). These results demonstrate that β-cell–specific IL-2 expression effectively suppresses ongoing autoimmunity long-term by enhancing the islet Foxp3$^+$Treg pool.

DISCUSSION

IL-2 is essential for the homeostasis of Foxp3$^+$Tregs, and dysregulation of the IL-2–IL-2R axis has been linked to aberrant Foxp3$^+$Treg survival and/or function in NOD mice and type 1 diabetic patients (9–12). Systemic administration of low-dose rIL-2 or IL-2–antibody complexes is effective in preventing ongoing β-cell autoimmunity in NOD mice (16,25–29). Nevertheless, achieving a protective versus proinflammatory response via systemic rIL-2 delivery can be problematic. For instance, systemic low-dose rIL-2 plus rapamycin resulted only in a transient increase in FOXP3$^+$Tregs in type 1 diabetic subjects, and β-cell function declined, suggesting exacerbated autoimmunity (30). Our results demonstrate that dsAAV vector–mediated targeting of IL-2 expression to β-cells is an effective strategy to manipulate the islet Foxp3$^+$Treg pool and diabetogenic response, while avoiding complications associated with systemic delivery of rIL-2.

A key finding made in this study was the differential effect of β-cell–specific IL-2 on islet-infiltrating Foxp3$^+$Tregs and Teffs (Fig. 2). Elevated local levels of IL-2 resulted in marked expansion of islet Foxp3$^+$Tregs but not Teffs. This observation is consistent with studies demonstrating that Foxp3$^+$Tregs are more sensitive to IL-2 compared with naive T cells and Teffs, partly due to constitutive expression of CD25 by Foxp3$^+$Tregs (45). Indeed, the level and frequency of IL-2R signaling as measured by pSTAT5 was significantly increased in islet Foxp3$^+$Tregs versus Teffs in dsAAV8mIP-IL2–treated NOD mice (Fig. 3). No effect of β-cell–specific IL-2 expression on PLN-resident Foxp3^{+-} Tregs was detected (Figs. 2 and 3), presumably due to β-cell secretion of low levels of IL-2 into the bloodstream and not the lymphatics. The increased number of islet Foxp3^{+-} Tregs correlated with enhanced proliferation early after dsAAV8mIP-IL2 treatment (Fig. 4*D*). Interestingly, islet Foxp3$^+$Tregs division was reduced compared with untreated animals 4 weeks post–dsAAV8mIP-IL2 vaccination (Fig. 4*D*). This result suggests that homeostasis is achieved overtime within the Foxp3$^+$Treg pool despite increased local levels of IL-2 and elevated IL-2R signaling (Fig. 3). Accordingly, long-term maintenance of islet Foxp3$^+$Tregs in dsAAV8mIP-IL2–treated animals (Fig. 5*C* and *D*) is likely due to enhanced survival, reflected by increased expression of anti-apoptotic Bcl-2 (Fig. 4*A*) and Bcl-xL (Supplementary Fig. 2) as opposed to persistent levels of elevated Foxp3$^+$Treg proliferation in the islets.

In addition to increasing the size of the pool, β-cell–specific IL-2 also induced qualitative changes in islet Foxp3$^+$Tregs. For instance, up to a four-fold increase in suppressor activity was detected in vitro by BDC peptide–specific islet Foxp3$^+$Tregs from dsAAV8mIP-IL2–treated NOD.BDC.Foxp3^{GFP} mice (Fig. 4*F*). The latter may be explained by the approximate two-fold increase in the frequency of CD62L^{HI} Foxp3$^+$Tregs in the islets of dsAAV8mIP-IL2–treated NOD mice (Fig. 2*C*). We and others (6,19,46,47) have reported that CD62L^{HI} versus CD62L^{LO} Foxp3$^+$Tregs exhibit increased suppressor activity and that elevated systemic levels of IL-2 promote expansion of CD62L^{HI} Foxp3$^+$Tregs in vivo. An increase in the general fitness of islet Foxp3$^+$Tregs, marked by elevated levels of CD25 and anti-apoptotic molecules for instance, may also contribute to more robust suppressor function. Enhanced islet Foxp3$^+$Treg suppression, however, did not correlate with elevated levels of IL-10 or transforming growth factor-β1 expression (data not shown).

Importantly, increases in islet Foxp3$^+$Tregs by β-cell–expressed IL-2 were sufficient to suppress ongoing β-cell autoimmunity at late preclinical stages and prevent the onset of diabetes long-term (Fig. 5*A* and *B*). Initial efforts to induce remission in recent-onset diabetic NOD mice by dsAAV8mIP-IL2 vaccination have proven to be unsuccessful (Supplementary Fig. 3). The latter may be due to an insufficient β-cell pool that can be transduced, thereby limiting local levels of IL-2 (Supplementary Fig. 3). It is noteworthy that the reduced ratio of Teffs to Foxp3$^+$Tregs and increased frequency of CD62L^{HI} Foxp3$^+$Tregs in the islets observed 4 weeks post–dsAAV8mIP-IL2 vaccination (Fig. 2) were also evident in NOD mice monitored for diabetes long-term (e.g., up to 23 weeks after dsAAV vaccination) (Fig. 5). This result is particularly striking in view of the progressive increase in the Teffs to Foxp3$^+$Tregs ratio, as well as the declining frequency of CD62L^{HI} Foxp3$^+$Tregs apparent in the islets of 35-week-old control NOD female mice (Fig. 5*D* and *E*), typical of ongoing β-cell autoimmunity. These findings demonstrate that once established, the islet Foxp3$^+$Treg pool is maintained long-term by persistent β-cell–expressed IL-2. Indeed, similar numbers of islet Foxp3$^+$Tregs were detected in NOD mice treated 23 (Supplementary Fig. 4) versus 4 weeks (Fig. 2*B*)

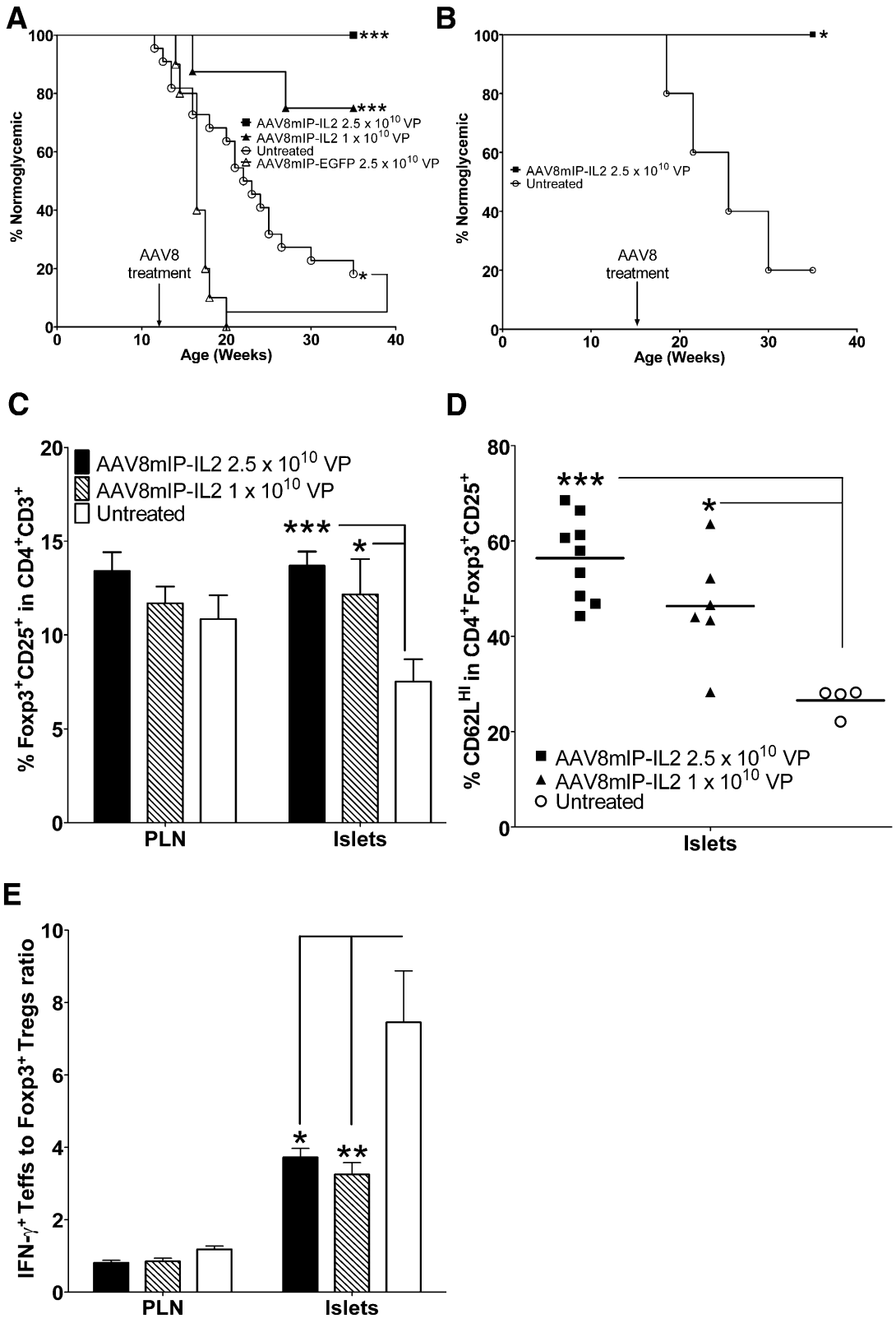

FIG. 5. dsAAV8mIP-IL2 prevents diabetes in NOD mice at late preclinical stages. *A*: Ten- to 12-week-old NOD female mice were treated with 2.5 × 10^{10} VPs (n = 9) or 1 × 10^{10} VPs (n = 8) of dsAAV8mIP-IL2, 2.5 × 10^{10} VPs of dsAAV8mIP-EGFP (n = 10), or left untreated (n = 22) and monitored for diabetes. *P < 0.05, ***P < 10^{-3}, Kaplan-Meier log-rank test. *B*: Fifteen- to 16-week-old NOD females were treated with 2.5 × 10^{10} VPs (n = 5) dsAAV8mIP-IL2 or were left untreated (n = 5) and monitored for diabetes as in *A*. *P < 0.05, Kaplan-Meier log-rank test. *C*: At 35 weeks of age, the frequency of Foxp3$^+$CD25$^+$CD4$^+$ T cells in the islets and PLNs of NOD mice from *A*. *P < 0.05, ***P < 10^{-3}, two-way ANOVA ± SEM. *D*: Islet Foxp3$^+$CD25$^+$CD4$^+$ T cells were assessed for CD62L expression. *P < 0.05, ***P < 10^{-3}, one-way ANOVA ± SEM. *E*: The ratio of IFN-γ$^+$ Teffs to Foxp3$^+$Tregs was compared between treatment groups in the PLNs and islets. *P < 0.05, **P < 10^{-2}, two-way ANOVA ± SEM.

post–dsAAVmIP-IL2 vaccination. Whether expression of β-cell–specific IL-2 is required to maintain islet Foxp3^{+} Tregs needs to be determined. Interestingly, dsAAV8mIP-IL2 failed to prevent diabetes in transgenic NOD.8.3 mice expressing the H2K^{d}-restricted T-cell receptor specific for islet-specific glucose-6-phosphatase catalytic subunit-related protein (Supplementary Fig. 5), suggesting that Foxp3^{+}Tregs are required for disease prevention; for instance, CD4^{+} Foxp3^{+}Tregs make up only <1% of the islet T cell pool following dsAAV8mIP-IL2 vaccination.

This study further highlights the efficacy of dsAAV vector–mediated gene transfer to selectively modify the immunogenicity of β-cells in vivo. Transduction of β-cells in vivo with a dsAAV vector results in rapid transgene expression that persists long-term (Fig. 1*B*); the latter indirectly demonstrating that β-cell viability and function are unaffected by dsAAV vector transduction. The use of an insulin promoter restricts transgene expression to β-cells, so that high local cytokine levels can be obtained within the islets and complications associated with systemic cytokine delivery minimized (30). A similar approach has been taken to target ectopic IL-4 expression to β-cells (35). Recent technological advances can also be exploited to refine β-cell specificity and reduce immunogenicity of AAV capsid proteins, thereby enhancing application of dsAAV vector gene transfer for the treatment of type 1 diabetes in the clinic (48).

Our observations are consistent with a model in which elevated local IL-2 has direct effects on islet Foxp3^{+}Tregs, only minimal (if any) on islet Teffs, and no effect on non–T cell islet residents such as NK cells and B cells (Supplementary Fig. 6). An increased pool of islet Foxp3^{+}Tregs characterized by a phenotypic shift toward CD62L^{HI} Foxp3^{+}Tregs and increased fitness and suppressor function effectively blocks ongoing β-cell destruction by Teffs. Once established, the islet Foxp3^{+}Treg pool is stable and long-term tolerance maintained. These results provide strong rationale to further pursue β-cell–specific targeting of IL-2 and other cytokines as a strategy to manipulate islet-resident Tregs and block the diabetogenic response.

ACKNOWLEDGMENTS

This work was supported by a grant from the National Institutes of Health (5R01-DK-081585). M.C.J. and A.L.G. were supported by a National Institutes of Health training grant (5T32-AI-07273).

No potential conflicts of interest relevant to this article were reported.

M.C.J., A.L.G., and S.C.N. researched data, contributed to discussion, and wrote and edited the manuscript. C.L., R.J.S., B.W., and R.T. contributed to discussion and wrote and edited the manuscript. R.T. is the guarantor of this work and, as such, had full access to all the data in the study and takes responsibility for the integrity of the data and the accuracy of the data analysis.

The authors thank Dr. Charles Kroger for critical reading of the manuscript.

REFERENCES

1. Anderson MS, Bluestone JA. The NOD mouse: a model of immune dysregulation. Annu Rev Immunol 2005;23:447–485
2. Bach JF. Insulin-dependent diabetes mellitus as an autoimmune disease. Endocr Rev 1994;15:516–542
3. Tisch R, McDevitt H. Insulin-dependent diabetes mellitus. Cell 1996;85:291–297
4. André I, Gonzalez A, Wang B, Katz J, Benoist C, Mathis D. Checkpoints in the progression of autoimmune disease: lessons from diabetes models. Proc Natl Acad Sci USA 1996;93:2260–2263
5. Brusko TM, Wasserfall CH, Clare-Salzler MJ, Schatz DA, Atkinson MA. Functional defects and the influence of age on the frequency of CD4+ CD25+ T-cells in type 1 diabetes. Diabetes 2005;54:1407–1414
6. Pop SM, Wong CP, Culton DA, Clarke SH, Tisch R. Single cell analysis shows decreasing FoxP3 and TGFbeta1 coexpressing CD4+CD25+ regulatory T cells during autoimmune diabetes. J Exp Med 2005;201:1333–1346
7. Tritt M, Sgouroudis E, d'Hennezel E, Albanese A, Piccirillo CA. Functional waning of naturally occurring CD4+ regulatory T-cells contributes to the onset of autoimmune diabetes. Diabetes 2008;57:113–123
8. You S, Belghith M, Cobbold S, et al. Autoimmune diabetes onset results from qualitative rather than quantitative age-dependent changes in pathogenic T-cells. Diabetes 2005;54:1415–1422
9. Fontenot JD, Rasmussen JP, Gavin MA, Rudensky AY. A function for interleukin 2 in Foxp3-expressing regulatory T cells. Nat Immunol 2005;6:1142–1151
10. Furtado GC, Curotto de Lafaille MA, Kutchukhidze N, Lafaille JJ. Interleukin 2 signaling is required for CD4(+) regulatory T cell function. J Exp Med 2002;196:851–857
11. Malek TR, Yu A, Vincek V, Scibelli P, Kong L. CD4 regulatory T cells prevent lethal autoimmunity in IL-2Rbeta-deficient mice. Implications for the nonredundant function of IL-2. Immunity 2002;17:167–178
12. Setoguchi R, Hori S, Takahashi T, Sakaguchi S. Homeostatic maintenance of natural Foxp3(+) CD25(+) CD4(+) regulatory T cells by interleukin (IL)-2 and induction of autoimmune disease by IL-2 neutralization. J Exp Med 2005;201:723–735
13. Granucci F, Feau S, Angeli V, Trottein F, Ricciardi-Castagnoli P. Early IL-2 production by mouse dendritic cells is the result of microbial-induced priming. J Immunol 2003;170:5075–5081
14. Sgouroudis E, Kornete M, Piccirillo CA. IL-2 production by dendritic cells promotes Foxp3(+) regulatory T-cell expansion in autoimmune-resistant NOD congenic mice. Autoimmunity 2011;44:406–414
15. Sgouroudis E, Albanese A, Piccirillo CA. Impact of protective IL-2 allelic variants on CD4+ Foxp3+ regulatory T cell function in situ and resistance to autoimmune diabetes in NOD mice. J Immunol 2008;181:6283–6292
16. Tang Q, Adams JY, Penaranda C, et al. Central role of defective interleukin-2 production in the triggering of islet autoimmune destruction. Immunity 2008;28:687–697
17. Yamanouchi J, Rainbow D, Serra P, et al. Interleukin-2 gene variation impairs regulatory T cell function and causes autoimmunity. Nat Genet 2007;39:329–337
18. Encinas JA, Wicker LS, Peterson LB, et al. QTL influencing autoimmune diabetes and encephalomyelitis map to a 0.15-cM region containing Il2. Nat Genet 1999;21:158–160
19. Goudy KS, Johnson MC, Garland A, et al. Reduced IL-2 expression in NOD mice leads to a temporal increase in CD62Llo FoxP3+ CD4+ T cells with limited suppressor activity. Eur J Immunol 2011;41:1480–1490
20. McGuire HM, Vogelzang A, Hill N, Flodström-Tullberg M, Sprent J, King C. Loss of parity between IL-2 and IL-21 in the NOD Idd3 locus. Proc Natl Acad Sci USA 2009;106:19438–19443
21. Long SA, Cerosaletti K, Bollyky PL, et al. Defects in IL-2R signaling contribute to diminished maintenance of FOXP3 expression in CD4(+)CD25(+) regulatory T-cells of type 1 diabetic subjects. Diabetes 2010;59:407–415
22. Malek TR. The biology of interleukin-2. Annu Rev Immunol 2008;26:453–479
23. Koreth J, Matsuoka K, Kim HT, et al. Interleukin-2 and regulatory T cells in graft-versus-host disease. N Engl J Med 2011;365:2055–2066
24. Saadoun D, Rosenzwajg M, Joly F, et al. Regulatory T-cell responses to low-dose interleukin-2 in HCV-induced vasculitis. N Engl J Med 2011;365:2067–2077
25. Goudy KS, Johnson MC, Garland A, et al. Inducible adeno-associated virus-mediated IL-2 gene therapy prevents autoimmune diabetes. J Immunol 2011;186:3779–3786
26. Grinberg-Bleyer Y, Baeyens A, You S, et al. IL-2 reverses established type 1 diabetes in NOD mice by a local effect on pancreatic regulatory T cells. J Exp Med 2010;207:1871–1878
27. Kornete M, Sgouroudis E, Piccirillo CA. ICOS-dependent homeostasis and function of Foxp3+ regulatory T cells in islets of nonobese diabetic mice. J Immunol 2012;188:1064–1074
28. Koulmanda M, Budo E, Bonner-Weir S, et al. Modification of adverse inflammation is required to cure new-onset type 1 diabetic hosts. Proc Natl Acad Sci USA 2007;104:13074–13079
29. Webster KE, Walters S, Kohler RE, et al. In vivo expansion of T reg cells with IL-2-mAb complexes: induction of resistance to EAE and long-term acceptance of islet allografts without immunosuppression. J Exp Med 2009;206:751–760

30. Long SA, Rieck M, Sanda S, et al.; Diabetes TrialNet and the Immune Tolerance Network. Rapamycin/IL-2 combination therapy in patients with type 1 diabetes augments Tregs yet transiently impairs β-cell function. Diabetes 2012;61:2340–2348
31. Grieger JC, Samulski RJ. Adeno-associated virus vectorology, manufacturing, and clinical applications. Methods Enzymol 2012;507:229–254
32. Simonelli F, Maguire AM, Testa F, et al. Gene therapy for Leber's congenital amaurosis is safe and effective through 1.5 years after vector administration. Mol Ther 2010;18:643–650
33. Maguire AM, Simonelli F, Pierce EA, et al. Safety and efficacy of gene transfer for Leber's congenital amaurosis. N Engl J Med 2008;358:2240–2248
34. Jiang H, Pierce GF, Ozelo MC, et al. Evidence of multiyear factor IX expression by AAV-mediated gene transfer to skeletal muscle in an individual with severe hemophilia B. Mol Ther 2006;14:452–455
35. Rehman KK, Trucco M, Wang Z, Xiao X, Robbins PD. AAV8-mediated gene transfer of interleukin-4 to endogenous beta-cells prevents the onset of diabetes in NOD mice. Mol Ther 2008;16:1409–1416
36. Wang Z, Zhu T, Rehman KK, et al. Widespread and stable pancreatic gene transfer by adeno-associated virus vectors via different routes. Diabetes 2006;55:875–884
37. McCarty DM, Monahan PE, Samulski RJ. Self-complementary recombinant adeno-associated virus (scAAV) vectors promote efficient transduction independently of DNA synthesis. Gene Ther 2001;8:1248–1254
38. Rehman KK, Wang Z, Bottino R, et al. Efficient gene delivery to human and rodent islets with double-stranded (ds) AAV-based vectors. Gene Ther 2005;12:1313–1323
39. Katz JD, Wang B, Haskins K, Benoist C, Mathis D. Following a diabetogenic T cell from genesis through pathogenesis. Cell 1993;74:1089–1100
40. Bettelli E, Carrier Y, Gao W, et al. Reciprocal developmental pathways for the generation of pathogenic effector TH17 and regulatory T cells. Nature 2006;441:235–238
41. Verdaguer J, Schmidt D, Amrani A, Anderson B, Averill N, Santamaria P. Spontaneous autoimmune diabetes in monoclonal T cell nonobese diabetic mice. J Exp Med 1997;186:1663–1676
42. Grieger JC, Choi VW, Samulski RJ. Production and characterization of adeno-associated viral vectors. Nat Protoc 2006;1:1412–1428
43. Wong CP, Stevens R, Long B, et al. Identical beta cell-specific CD8(+) T cell clonotypes typically reside in both peripheral blood lymphocyte and pancreatic islets. J Immunol 2007;178:1388–1395
44. Wang Z, Zhu T, Qiao C, et al. Adeno-associated virus serotype 8 efficiently delivers genes to muscle and heart. Nat Biotechnol 2005;23:321–328
45. O'Gorman WE, Dooms H, Thorne SH, et al. The initial phase of an immune response functions to activate regulatory T cells. J Immunol 2009;183:332–339
46. Ermann J, Hoffmann P, Edinger M, et al. Only the CD62L+ subpopulation of CD4+CD25+ regulatory T cells protects from lethal acute GVHD. Blood 2005;105:2220–2226
47. Szanya V, Ermann J, Taylor C, Holness C, Fathman CG. The subpopulation of CD4+CD25+ splenocytes that delays adoptive transfer of diabetes expresses L-selectin and high levels of CCR7. J Immunol 2002;169:2461–2465
48. Asokan A, Schaffer DV, Samulski RJ. The AAV vector toolkit: poised at the clinical crossroads. Mol Ther 2012;20:699–708